MULTI-TEMPORAL DEM AND LAND USE ANALYSIS FOR DETERMINING GULLY FORMATION

A Thesis submitted to the faculty of
San Francisco State University
In partial fulfillment of
the requirements for
the Degree

Master of Science

In

Geographic Information Science

by

Charles Brandt Bates

San Francisco, California

May 2019

Copyright by
Charles Brandt Bates
2019

CERTIFICATION OF APPROVAL

I certify that I have read Multi-temporal DEM and Land Use Analysis for Determining Gully Formation by Charles Brandt Bates, and that in my opinion this work meets the criteria for approving a thesis submitted in partial fulfillment of the requirement for the degree Master of Science in Geographic Information Science at San Francisco State University.

Leonhard Blesius, Ph.D.
Associate Professor of Geography

Jerry Davis, Ph.D.
Professor of Geography

MULTI-TEMPORAL DEM AND LAND USE ANALYSIS FOR DETERMINING GULLY FORMATION

Charles Brandt Bates
San Francisco, California
2019

Soil erosion has become a serious concern for the Pescadero Watershed in San Mateo County. Since the late 19th century, extensive gully networks have formed due to human land use such as cattle grazing and agriculture. Excess sediment from gullies impairs aquatic habitats and the stream system's ability to carry flood waters. This study presents a group of methods that can be used to indicate the status of gully network change in the Pescadero Watershed. Remote sensing techniques are beneficial because they can minimize the time needed for more traditional ground survey methods. Digital Elevation Models (DEMs), from relatively recent LiDAR datasets, were used in change detection models or DEMs of Difference (DoD). This study developed a contemporary DEM for 2018 using Structure-from-Motion (SfM) photogrammetry, which is an approach using a series of unordered images. This produced a high-resolution elevation model as well as an RGB orthomosaic image for two-dimensional analysis. Since regional gully networks primarily consist of barren soil, the SfM method is particularly successful in gathering elevation data that highlights erosion patterns. In addition, grid elevations in each successive DEM were subtracted from the more recent DEM to produce maps that show areas of deposition, erosion, or no change. In these models, negative values represent areas of erosion, and positive values represent areas of deposition. Based on the Root Mean Square Error (RMSE) of each DEM, a Minimum Level of Detection (LoD_{min}) highlighted areas of significant elevation change. The study found that results were highly dependent on the LoD_{min} where DEMs with lower errors participating in a DoD provided results with a higher level of detail and confidence. SfM techniques yielded the most accurate results, especially with their ability to detect finer-scale erosion and vertical accuracy. In order to analyze finer-scale bank erosion, the study incorporated two-dimensional analysis using

aerial imagery and an object-based image segmentation workflow. The classification result from the image segmentation output was successful in delineating a barren soil class representing gullies as objects for 2001. Given the relatively small study site (3.27 ha), manual digitizing methods were used where three-dimensional analyses was not feasible. This study concluded that combining a DEM derived from SfM and DEMs from LiDAR in a DoD, provided information to determine gully geomorphic change. This information will ideally guide resource management practices for the Pescadero Watershed and encompassing areas affected by gully erosion.

I certify that the abstract is a correct representation of the content of this thesis.

_____ _____

Chair, Thesis Committee Date

ACKNOWLEDGEMENTS

I wish to thank the San Mateo County Resource Conservation District for providing elevation data and logistical support during field work. I also thank Tim C. Best for assisting me in conceptualizing this project. Thanks to Prof. Leonhard Blesius and Prof. Jerry Davis for their work as my thesis committee.

TABLE OF CONTENTS

LIST OF TABLES

Table Page

LIST OF FIGURES

Figures Page

1 Introduction

Gullies are the result of a specific erosional process where concentrated water flows recur in narrow channels, eroding sharply into the soil. It eventually creates steep banks that can range from depths of 0.5 m to 25 m. This type of landform resembles knife-like cuts, typically occurring on hillslopes. Gully formations supply soil runoff into streams, with sediment production increasing as the gully system evolves over time (Marden et al., 2012). These erosional features are too deep to easily repair with ordinary tilling equipment.

Previous studies by Conforti et al. (2011) and Zucca et al. (2006) have investigated reasons for gully formation, but there is a lack of suitable methods for observing the status of gullies - stabilization and/or growth. Light Detection and Ranging (LiDAR) has been used for detailed mapping of complex gully morphology and their soil erosion patterns. The advantages of LiDAR compared to satellite imagery interpretation and field surveying techniques are primarily: (a) high vertical and horizontal accuracy at a regional scale, (b) better elevation data acquisition in forested areas, and (c) higher data density (Vendrusculo, 2014). However, LiDAR datasets are not always publicly available for remote or rural areas, because it can be costly to coordinate flyovers and process large datasets. Therefore, LiDAR may not be the most promising approach for short-term monitoring of gully erosion.

The objective of this study is to evaluate a group of methods for fast, effective and efficient analysis of gullies. This group of methods includes the use of historic aerial

photography, available LiDAR datasets, and Structure-from-Motion (SfM) photogrammetry to document not only areal changes, but also detect vertical differences by creating Digital Elevation Models (DEMs). These DEMs can then be used to classify gully areas as active erosion, deposition or stabilized at a sub-meter resolution. While implementing erosion improvements for an entire gully system can be costly and ineffective, this information can be used to identify specific areas of active erosion within a larger gully system. This will better guide land stewardship priorities for erosion control and water quality measures, saving time and funding for resource management agencies.

1.1 Study area

The Pescadero Watershed is located along California's coastline, approximately 80 km south of San Francisco (Fig. 1). The watershed is comprised of two main streams, Pescadero Creek and Butano Creek, which drain into the Pescadero Marsh.

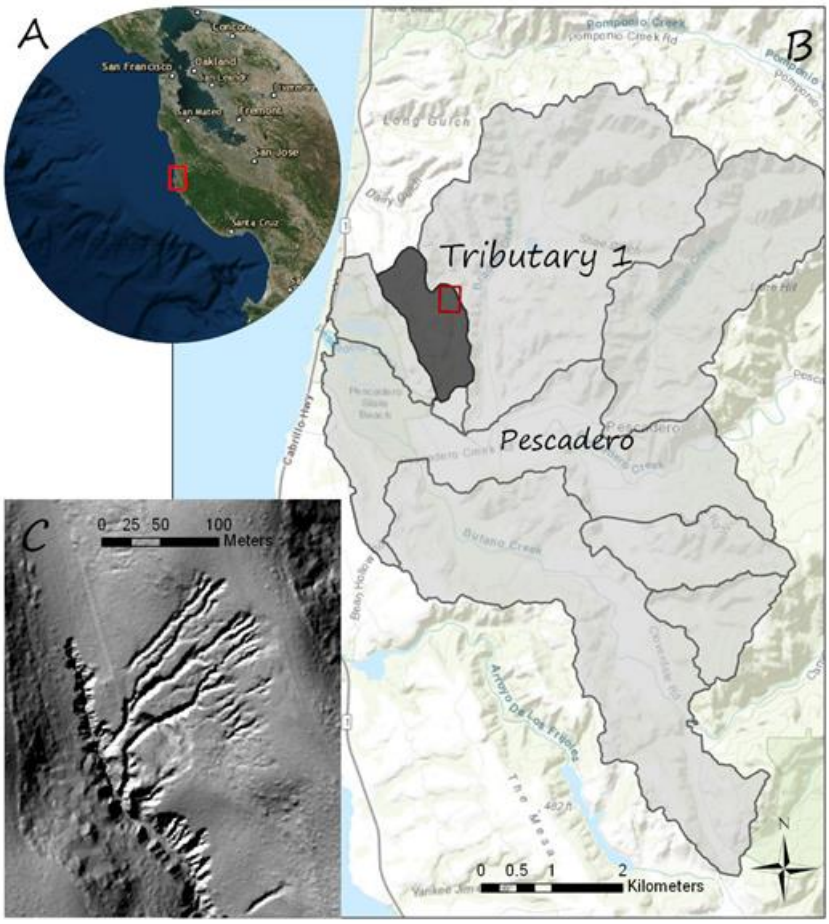

Fig. 1 Location of study's gully system. (A) Satellite image showing the study area in the context of central-northern California. (B) Location of gully system (red rectangle) in Tributary 1 (shaded area) of the Pescadero Watershed. (C) Hillshade dataset of the study site.

The Pescadero Watershed is experiencing unprecedented rates of erosion (Environmental Science Associates et al., 2004). In his study on the Pescadero-Butano Watershed sediment total maximum daily load, Frucht (2013) observed that a combination of intensive land management activities such as agriculture and grazing

along with proximity to the ocean, steep hillslopes, aspect, and lithology largely contribute to gully formation and susceptibility. The specific study area is located on a southwest facing, steep hillslope (Fig. 2). Today, it is primarily grassland and shrub cover with continued grazing (Frucht, 2013).

Fig. 2 View of gully arm on the southwest slope of the study site.

The majority of the western side of the watershed, west of the San Gregorio Fault, is categorized as a hillslope geomorphic unit (HGU), consisting of Quaternary and upper Tertiary sediments on moderate to steep slopes (Environmental Science Associates et al., 2004). Geologic units associated with the HGU and present at the study site consist of two Colma sandy loam or sand dune/beach deposits (Qs) (different slope severities), and the Tahana member of the Purisima Formation (Tpt) (Fig. 3) (USDA, 2017).

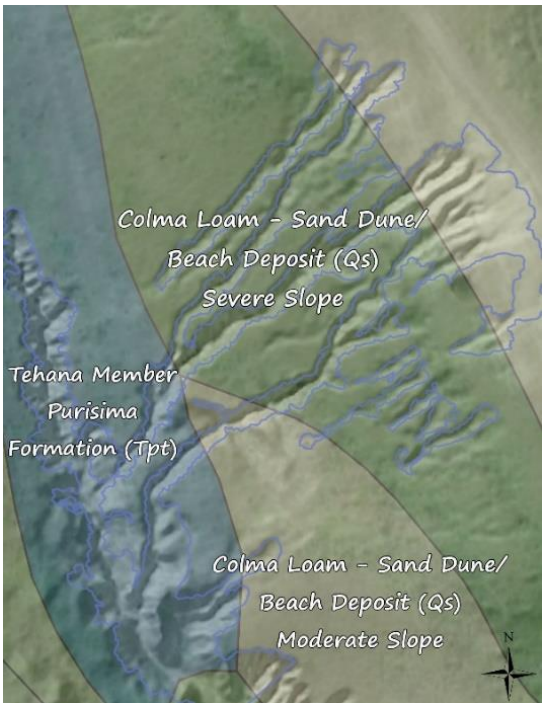

Fig. 3 Geologic map showing distribution of two Colma Loams, based on slope severity, and the Tehana Member of the Pursima Formation (USDA, 2017).

Once exposed, these light and friable rock types break down quickly into a fine sediment (Owens, 2003). The Qs deposit with its fine-grained particle size and sandy characteristics makes it particularly vulnerable to erosion. The Tpt erodibility is considered moderate and shows no severe signs of erosion in forested areas, but there is significant sheetwash erosion on grazed and moderate to steep hillslopes (Brown, 1973).

Slope and aspect play a major role in gully formation. In Spreiter's (1979) thesis on factors affecting gully formation and distribution in coastal San Mateo County, he identified south and west-facing slopes, characterized by grass and sparse shrub

vegetation, as more susceptible to gully formation. This may be due to more direct sunlight and less favorable moisture supply resulting in a relatively poor leached soil with higher concentrations of (Na^+).

Historically, the Pescadero Watershed was heavily forested. However, it experienced a habitat type-change due to agriculture, logging and extensive grazing practices in the late 19th and early 20th centuries. The Redwood City Times and Gazette reported in 1876 that flax seed cultivation was attractive to Pescadero farmers because they could arrange pre-season contracts with San Francisco-based linseed oil manufacturers (Redwood City Times and Gazette, 1876). Between the years of 1878 and 1880, the total acreage of flax seed grew from 72.8 ha to 1618.7 ha. Because flax cultivation requires fine homogenous topsoil, tilling on steep hillslopes can lead to small erosional channels, or rill development. Based on historical aerial photos from 1941 to 1976, the site was regularly plowed in order to eliminate rill expansion. However, due to the severe hillslope conditions, the rills developed into gullies, making them difficult to control with grading and plowing methods.

Gully formation was not solely associated with the use of agriculture on coastal hills, but also attributed to large storm events that coincided with the abandonment of agriculture (Swanson, 1989). These storms, along with normal rainfall, continue to deepen the gullies. The Pescadero watershed receives nearly all 63.5 cm of its average annual rainfall between the months of October and April. This rainfall delivers excess sediment into downstream aquatic habitats. The surplus of sediment negatively affects

aquatic habitat by impairing the stream's ability to carry floodwaters (Resource Conservation District, San Mateo, 2017). Excessive sediment from soil erosion is also the primary factor limiting habitat for steelhead trout. Excess fine sediment degrades fish spawning (Lal et al., 1999).

Pacific Watershed Associates, as part of the *Pescadero Watershed Assessment* (2004), conducted a study using aerial photo analysis of large landslides and gullies throughout the Pescadero Watershed. The study also included a field inventory of 40 randomly selected 16.2 ha [40-acre] parcels to measure past sediment delivery, estimation of total basin erosion and sediment delivery based on randomly selected sample plots, a combination of plot data and air photos to determine erosion rates, and an analysis of the percentage of past erosion that was anthropogenic or potentially controllable. Based on the study's results, 7,461,504 m^3 [8,160,000 yd^3] of sediment delivery was associated with human land use. This accounted for 91% of the watershed's 8,216,341 m^3 [8,985,500 yd^3] total sediment delivery entering stream channels from 1937 to 2002 (Pacific Watershed Associates, 2004).

2 Methods

2.1 LiDAR

DEMs from the 2006 and 2017 San Mateo County LiDAR terrestrial survey were used. The original LiDAR point cloud for San Mateo County was based on a USGS QL2 Base Specification, equating to four points per square meter. The County of San Mateo

Geographic Information Systems (GIS) Team generated DEMS from the survey's original .las point cloud file using Inverse Distance Weighting (IDW) interpolation function to a grid size of 0.3 m (San Mateo County Information Services Dept., 2017). The IDW tool uses a distance weighting function to interpolate a value for a raster grid, where a data point within a defined radius that is closer to the center of the grid receives higher weighting than data that is further away (Taylor et al., 2018).

2.2 Structure-from-motion

A surface model, representing current elevations of the study site, was created using structure-from-motion photogrammetry. SfM is a method to produce surface models from an unstructured and unordered series of images and was developed in the field of computer vision. Early applications created 3D models from images collected from the Internet for virtual tourism (Snavely et al., 2008). Dissimilar from traditional stereo-pair photogrammetry, SfM does not use precise camera location information in order to produce surface models (Christian and Davis, 2016). SfM matches many images concurrently. Features that have distinct edges with multiple directions are used to detect similarities from one image to the next.

2.2.1 Image acquisition

An advantage of using SfM for surface modeling is the low cost of required equipment. Aerial imagery was acquired with a DJI Phantom 4, an unmanned aerial vehicle (UAV) that is popular and easy to fly and includes a camera (1" CMOS 20 Mpixel 100-12800 ISO, FOV 84° 8.8 mm (24 equiv.) f/2.8-f/11, autofocus) on a gimbal. A total of 252 images were captured. Since this process collects many images, a lower quality camera could have been used (Westoby et al., 2012). However, a higher-grade camera inherently increases accuracy.

In their study on hillslope gully photogeomorphology, Christian and Davis (2016) noted that a SfM survey collected at a relatively low altitude (e.g. 30m) might provide more detailed gully information than a typical aerial LiDAR survey from a much higher platform. In order to consider the study site's slope disparities and to avoid image distortion, two flights were performed at different elevations (Fig. 4). The western half of the study site was comparatively flat at a lower elevation, ranging in slopes of 5-12 degrees. The eastern half of the study site was much steeper, with slopes as high as 42 degrees. Bank slopes within gully channels were as steep as 82 degrees.

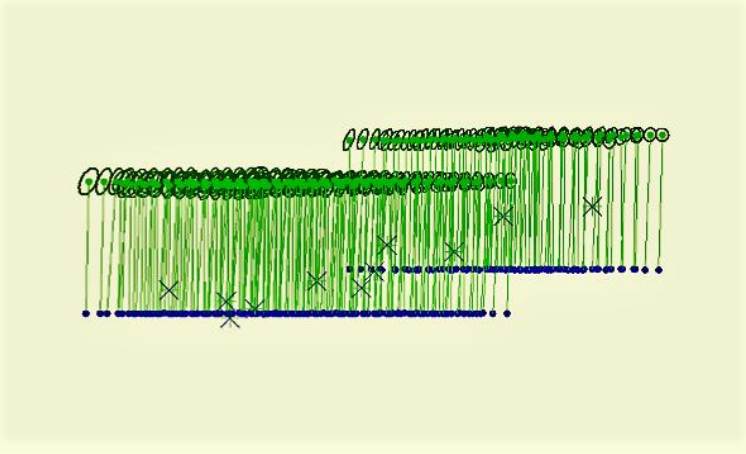

Fig. 4 Schematic from Pix4D showing the relative heights of each flight, image capture locations (green ovals) and GCPs (black x's).

2.2.2. Ground control points and checkpoints

In order to tie the images to their accurate location and create an elevation model, two initial global positioning system (GPS) tie points were collected in the field using a GeoHx6 and Zephyr Antenna. The two GPS points were positioned on the study area's edges, one on the southwestern edge and the other on the northeastern edge. These points were post-processed using a nearby base station, resulting in a 0.025 m accuracy.

Once the northing and easting values were established for the two initial points, sixteen points of known coordinates in the study area (GCPs) were surveyed. Although the original unmanned aerial system (UAS) imagery stores geolocation, the GCPs increase the absolute accuracy of the project, placing the surface model output at a more precise location. Due to the severe slope of the study site, and to prevent skewness during

the linear transformation, a relatively large set of GCPs were distributed across the study site (Fig. 5).

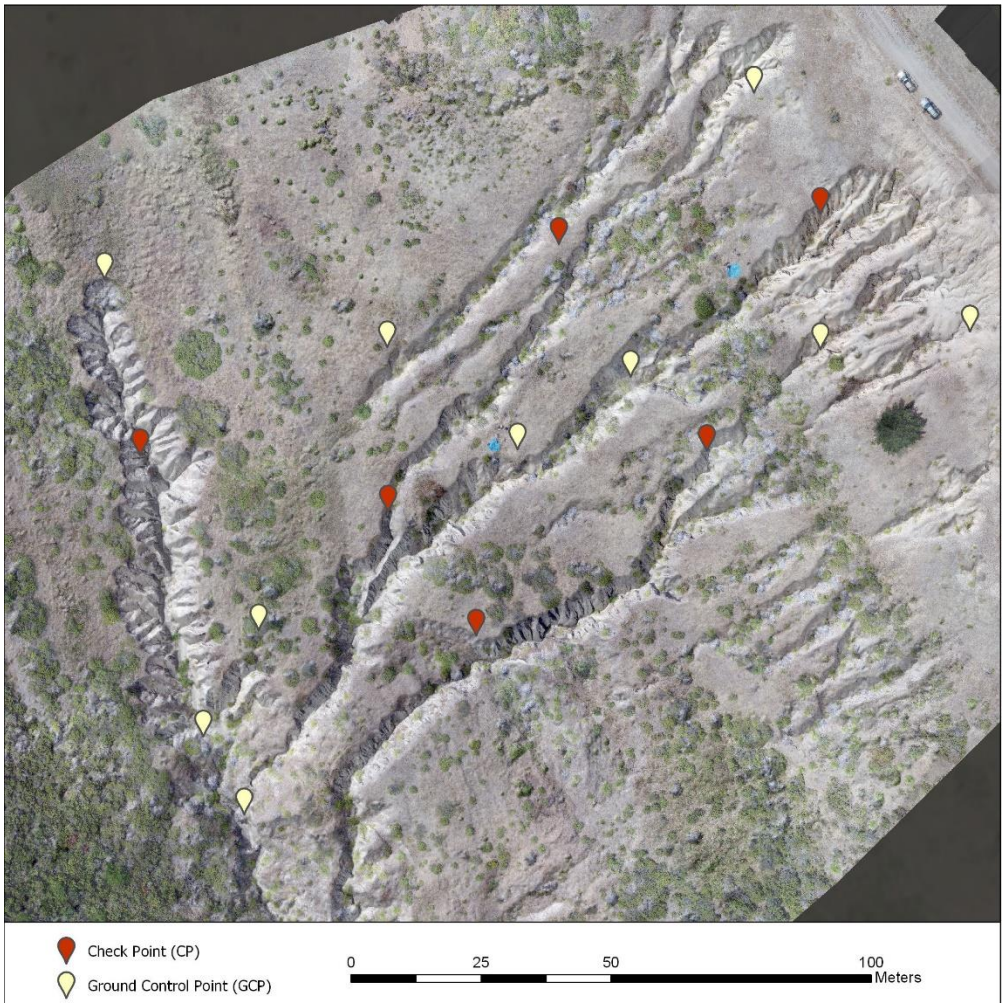

Fig. 5 Map of study site showing locations of CPs and GCPs. Blue dots are UAV takeoff and landing tarps.

Both ceiling tiles with black crosshairs and compact discs were used to mark the GCP survey locations. The ceiling tiles helped with manually locating the points in the

UAS imagery. Once these initial points were located in the imagery, nearby GCPs marked with discs were clearly visible. For the most accurate representation of elevation and direction, a Leica Builder 503 Total Station, with a 3" accuracy for horizontal and vertical angles, was used to survey each GCP. Similar to Westoby et al. (2012), the most time-consuming component was the establishment of GCPs in the field.

Five of the sixteen GCPs were used as checkpoints (CPs) in order to assess the absolute accuracy of the model. These points did not participate in the linear transformation of the model and were solely used to represent the relative RMSE of the DEM derived from SfM (Tbl. 1).

Check Point Name	Error X [m]	Error Y [m]	Error Z [m]	Projected Error [pixel]
5	0.0624	0.0322	0.0710	0.3599
6	-0.0625	-0.0156	-0.0813	0.7807
13	-0.0296	-0.0306	0.1486	0.8577
17	-0.0418	0.0820	-0.0032	0.5583
19	0.0507	0.1174	0.0860	0.4753
Mean [m]	-0.004175	0.049349	0.044220	
Sigma [m]	0.050800	0.045970	0.079194	
RMS Error [m]	0.050971	0.067443	0.090704	

Table 1. The difference between the initial and the computed position of the CPs showing the estimation of the absolute accuracy of the SfM 2018 DEM.

2.2.3. Point cloud editing using the RayCloud

With any SfM method for building an elevation model, two-dimensional pixels from imagery, in this case UAS photos, are transformed into three-dimensional voxels or cubic pixels (Christian and Davis, 2016). This transformation mimics human vision but is

constructed from hundreds, or even thousands, of images rather than just two to establish the location of a feature relative to all other matched features (Ni et al., 2010).

In this phase, Pix4D generated a densified point cloud and automatically assigned each data point to one of the following predefined groups: ground, road surface, high vegetation, building or human-made object. Group assignment or point classification required training samples that were based on geometry and color information. This automated Pix4D process is based on an algorithm using rural and low vegetated training dataset. The process performed well for the study site however, the output required slight manual refinement.

This stage initially produced a digital surface model (DSM). For analyzing geomorphological change, the DSM was further processed to create a DEM free of vegetation and manmade objects. Extraneous points that were clearly errors or classified as vegetation were manually removed from the point cloud. Examples of vegetation features (Fig. 6) included coyote brush (*Baccharis pilularis*) and jubata grass (*Cortaderia selloana*).

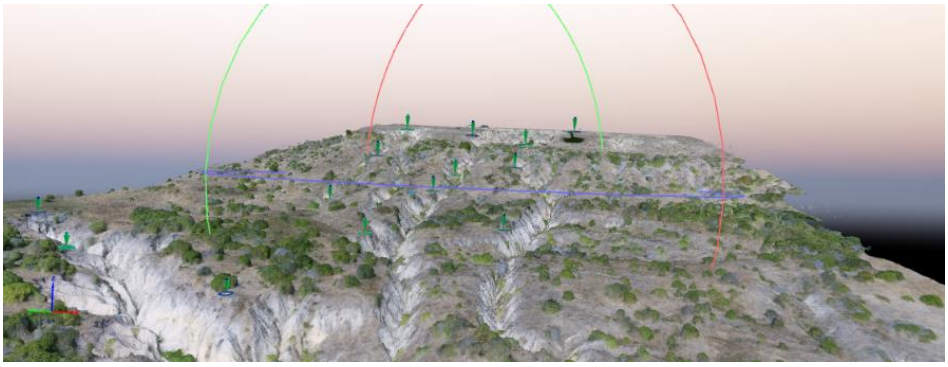

Fig. 6 Image of DSM based on automated point cloud classification, before vegetation removal in Pix4D RayCloud editor.

Using training samples and manual RayCloud editing, this step produced a ground classification group. All points participating in the ground and road surface class were used to generate a DEM (Fig. 7); the rest of the classes were disregarded.

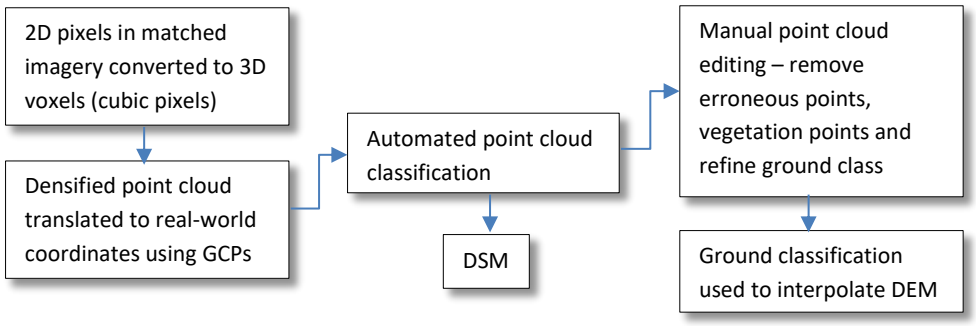

Fig. 7. Workflow for densified point cloud editing and SfM DEM.

2.3 DEM of difference and minimum level of detection

When multi-temporal DEMs are available, geomorphic change in time is inferred by DEM of Difference (DoD) grids, in which the elevation difference between old and new surfaces, hence erosion and deposition, is computed at the cell scale (Lane et al., 2003, Wheaton et al., 2010). DoDs can be particularly useful for quantifying hillslope erosion in semiarid regions (Coe et al., 1997), where field measurements of sediment transfer are usually difficult due to the low frequency and localized occurrence of rainfall events.

DEMs were subtracted on a cell-by-cell basis producing raster elevation models of difference. Datasets employed in the analysis included the 2018 DEM produced from SfM, and two DEMs (2006 and 2017) from San Mateo County Terrestrial LiDAR surveys (Fig. 8).

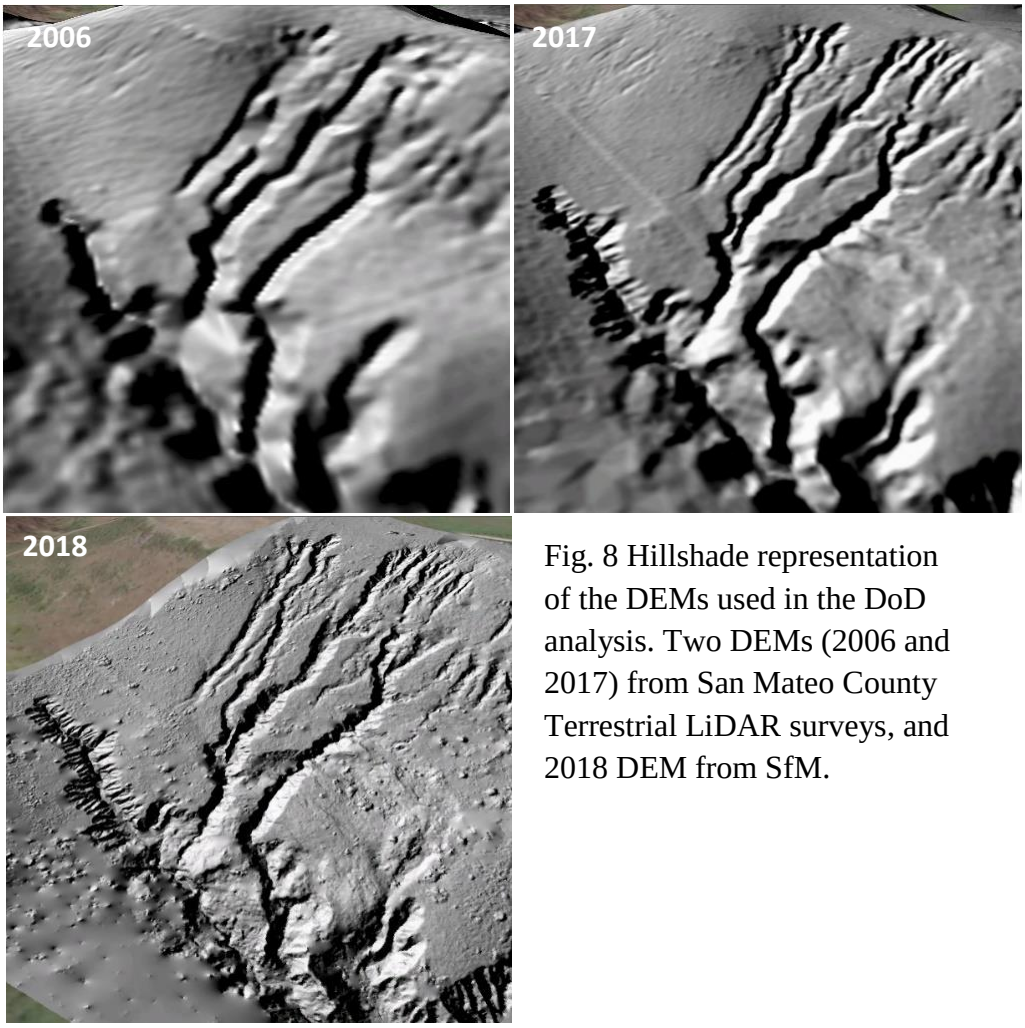

Fig. 8 Hillshade representation of the DEMs used in the DoD analysis. Two DEMs (2006 and 2017) from San Mateo County Terrestrial LiDAR surveys, and 2018 DEM from SfM.

Each change-model was made in ArcGIS Pro using the 3D Spatial Analyst raster math function, subtracting the DEM grid values for the later survey from the younger survey. The change in elevation can be represented as:

$$DoD = DEM_{new} - DEM_{old} \quad (1)$$

where a positive change at the cell level indicates sediment deposition and a negative change between survey years represents erosion.

Eq. (1) assumes that both DEMs are free of error and represent true on-the-ground conditions. However, as described by Wheaten et al. (2010), DEM elevations are likely to have some degree of vertical error. This consideration creates a more dependable DoD. Therefore, the error for each DEM was based on a RMSE value, indicating the model's vertical accuracy. The cumulative error in a DoD, or Minimum Level of Detection (LoD_{min}), can be estimated based on the root sum square of errors:

$$LoD_{min} = \sqrt{(\delta z_{new})^2 + (\delta z_{old})^2} \quad (2)$$

where δz_{new} and δz_{old} are the errors for DEM_{new} and DEM_{old} respectively. The LoD_{min} was applied to the entire DoD as an absolute threshold. Therefore, elevation change in the DoD must be greater than the LoD_{min} in order to signify dependable change.

2.4 Two-dimensional analysis

Aerial imagery was acquired from the University of California, Santa Cruz Library Aerial Photographs Digital Collections. The historical aerial images from years 1943, 1956, 1970, 1982, 1994 and 2001 were scanned into .tiff format using an EPSON Expression 1100XL scanner at a resolution of 1200 dpi. The .tiff files were then georectified in ArcGIS Pro based on a spline transformation using common reference points. With this method, it was possible to measure horizontal or two-dimensional gully change, rather than changes in gully depths using DoD analysis. This was used for observing changes in gully widths and rates of gully headcut erosion. A headcut is located at the uphill end of a gully and is typically very steep. As water passes over the headcut, bank erosion occurs, causing it to migrate upstream (Weaver et al., 1994). The historic imagery also provided valuable indication of the study site's land use management, vegetation cover and gully development.

DEMs were derived from the historic stereo pairs. Stereo pairs were selected based on their scale, resolution and available flight data. Examples of flight data include camera focal length, flight height and fiducial coordinates. However, the RMSE of the DEM outputs created in ERDAS Imagine were too high. Therefore, these models were unable to detect any significant elevation change.

It was difficult to manually detect gully edges in the historical imagery without a high degree of uncertainty. Delimiting gully edges manually resulted in an underestimation of gully width due to shadow. However, in some of the imagery years, particularly 2001, unique reflectivity of the barren soil could be used as training samples for image segmentation. In the case of older imagery with decreased resolution, finer gully edges within complex gully systems can be identified semi-automatically (Shruthi et al., 2011). Segmentation and classification tools provided an approach for extracting gully features from the imagery based on objects. Built on the image segmentation process, nearby pixels with similar spectral values were grouped together to create objects (ESRI, 2018). In doing so, this approach considered blurry gully edges and shadows. Before processing the imagery, training samples were set to establish the desired classification based on color reflectivity. As shown in figure 9, this approach was sufficient in delimiting the study site's gully network extent in 2001.

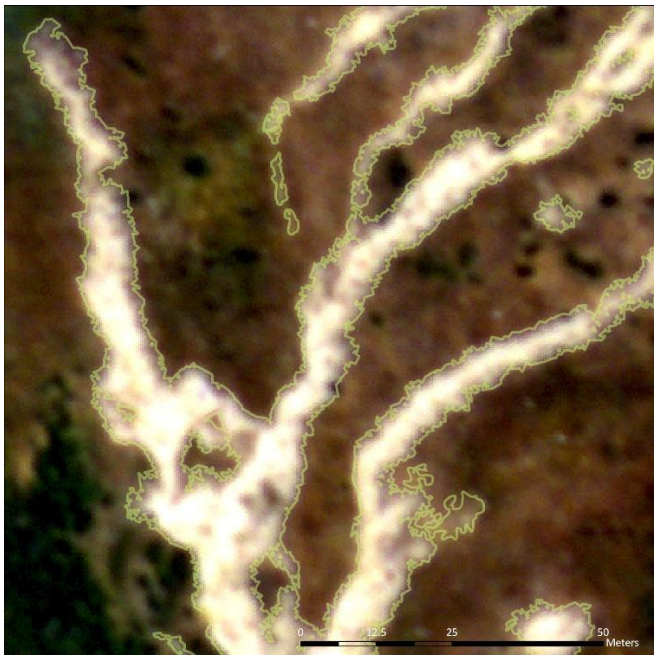

Fig. 9 Image displaying 2001 aerial image and image segementation results.

Using the SfM 2018 orthomosaic (0.025 m resolution), edges of the gully network were manually digitized. The perimeter was drawn in ArcGIS Pro, applying a 30 percent transparency filter to the orthomosaic in combination with the SfM 2018 DEMs grayscale hillshade as the base layer.

3 Results

Results detected an area of newly developed erosion in addition to areas that have stabilized since 2001. The accuracy of the segmented image output was 0.3 m.

Throughout the duration of the historical imagery years, the west gully channel expanded uphill, showing a gully headcut at the rate of 0.88 m/yr from 2001 to 2018 (Fig 10).

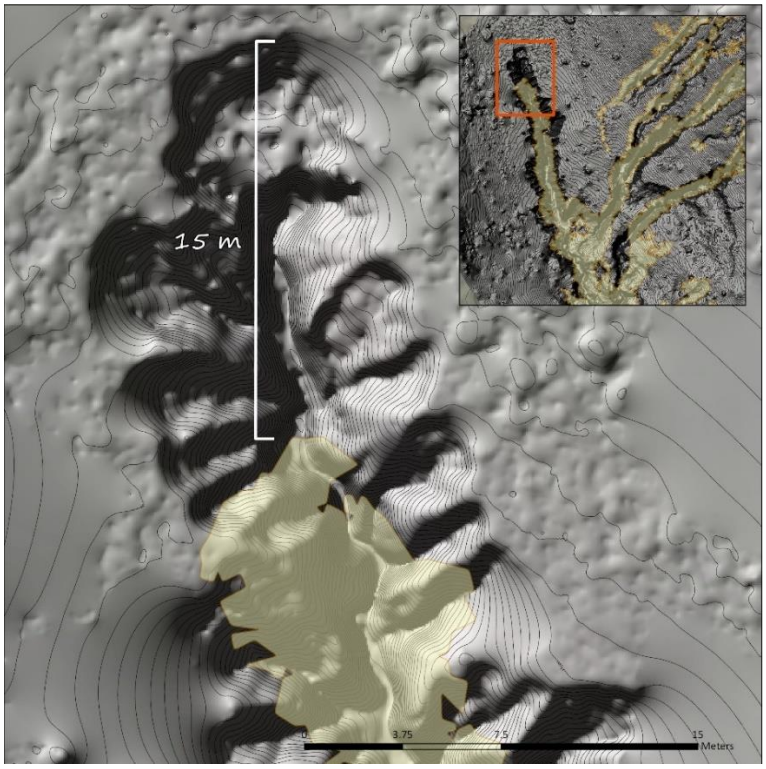

Fig. 10 Map of main gully headcut representing an erosion rate of 0.88 m/yr from 2001 (yellow) to 2018 (DEM basemap).

Headcuts also appeared to be the result of concentrated flow input from the connected southwest facing hillslope gullies. Due to steep hillslope conditions and lack of vegetation, rills started to develop in the early 1940s on the southwest facing slope. Based on historical image interpretation, these smaller erosional features were routinely harrowed but eventually became too large and deep to manage. By the late 1970's,

attempts to control the severe erosion were abandoned, resulting in deep, incised gully features.

The SfM approach was able to achieve a 0.06 m cell size for the DEM output with a vertical error of 0.09 m. The 2017 DEM presented an error of 0.71 m whereas the 2006 DEM error was significantly lower at 0.33 m (Kelley and Loecherback, 2006). Results showed that the San Mateo County DEM errors inherently influenced the LoD_{min}. For example, the LoD_{min} for the 2006-2018 DoD (Fig. 11) was 0.35 m. As geomorphic change increases with time, a lower LoD_{min} can detect finer erosion and deposition events that occur within one year rather than ten years. This is consistent with the concept that change detection is more reliable when measured elevation change is of a greater magnitude than associated DEM errors (Williams, 2012).

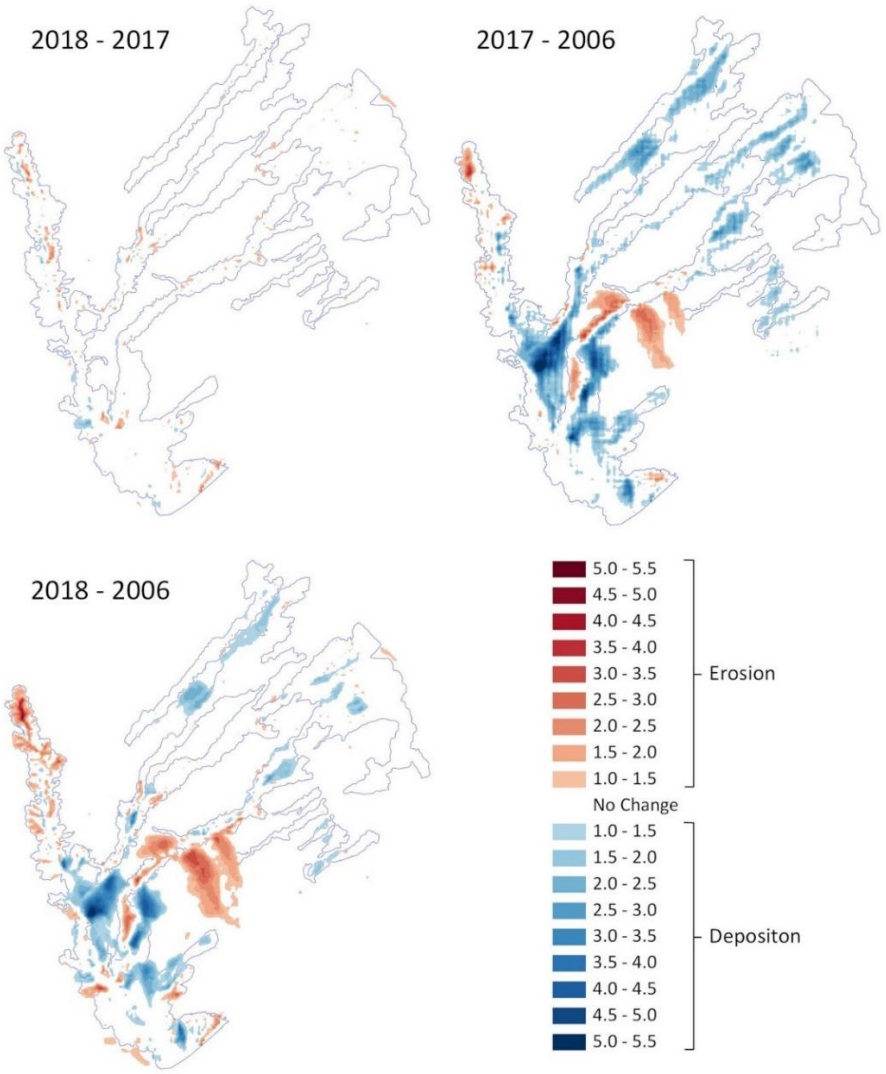

Fig. 11 DoDs incorporating level of detection thresholds (LoD_{min}). Red shows negative values (erosion), whereas blue shows positive values (deposition). All other areas are considered statistically unchanged.

Figure 12 is a detailed look at the 2018-2006 DoD. Area A demonstrates the model's ability to indicate active gully headcuts. A feature seen in connection with the headcut is a deepening channel from concentrated flows. This area is an active site of

erosion. The model illustrated patterns of erosion and deposition, where erosion typically occurs upstream and sediment collects downstream. This process is most apparent in area E where there is a convergence of contributing gully runoff as well as the drainage for the

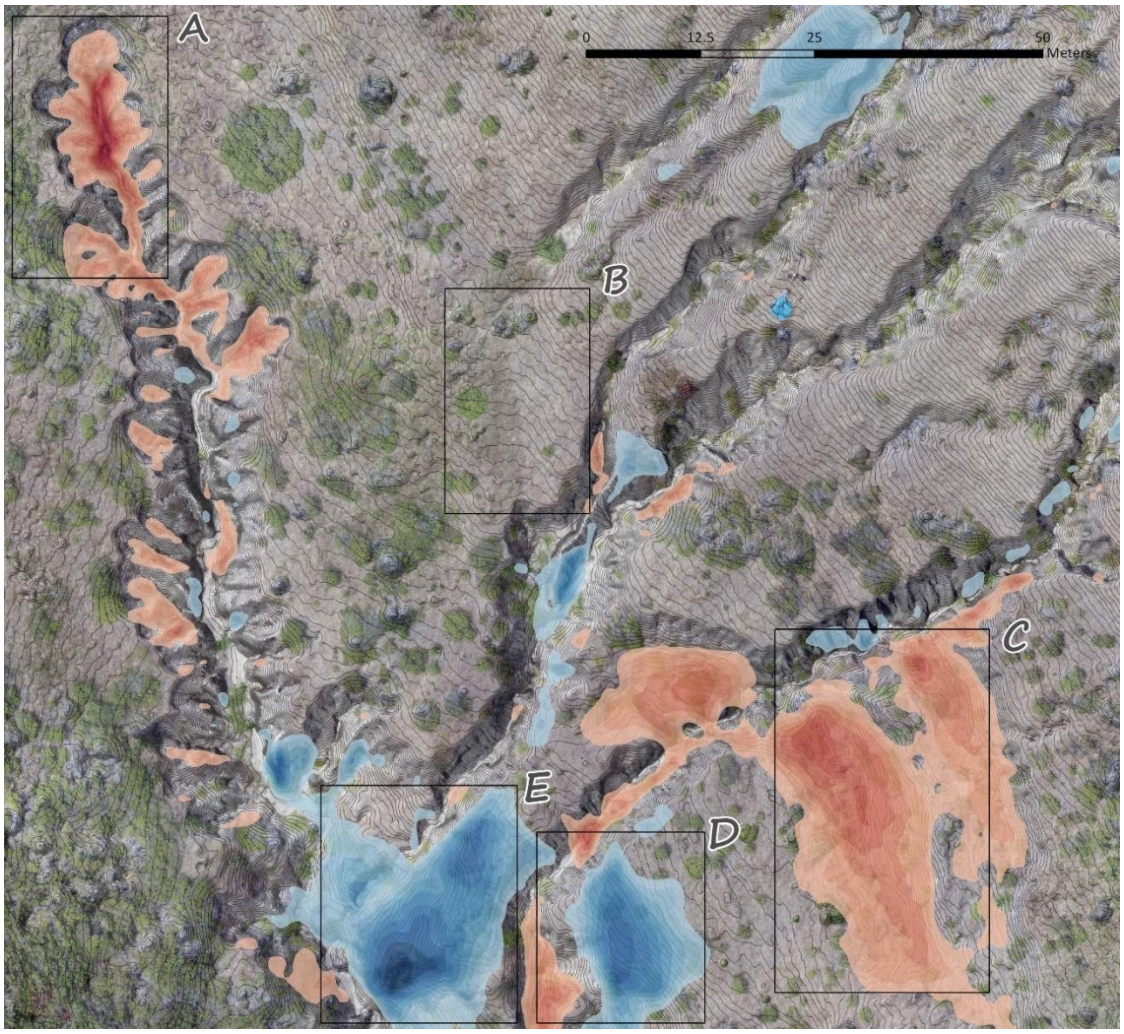

Fig. 12 Detailed results for the 2018-2006 DoD, where red indicates areas of erosion and blue indicates areas of sedimentation. (A) Erosion from gully headcut; (B) concave area that is stable and unchanged; (C) negative elevation change from slump and uphill scarp; (D) abandoned gully segment and new gully channel; and (E) positive elevation change in sediment collection area.

entire southwest facing slope. This collection area was confirmed through ground-truthing. Directly adjacent to area E, area D demonstrates a segment of the gully that had been redirected. This was the result of the downhill bank collapsing, thereby eroding a new channel. Based on the 2001 image segmentation output, this area was previously classified as barren soil and actively eroding. Since then, the channel has been cut off from concentrated water flow, allowing it to revegetate and reach a stable state.

In addition to highlighting soil erosion dynamics within the defined gully network, methods from this study could indicate less apparent erosional processes outside of the manually digitized 2018 boundaries of the gully. Area C is the site of a hillside mass movement, specifically, a slump. The uphill slope of the slump has some degree of exposed earth indicating a scarp; however, the majority of the surface is vegetated. Highlighted in Fig. 12, the slump moved in a vertical direction as a coherent unit. Based on these results, the DoD analysis conveyed a range of erosional processes. According to the 2006-2018 DoD statistics, the gully system had an average erosion of 0.22 m (Fig. 13).

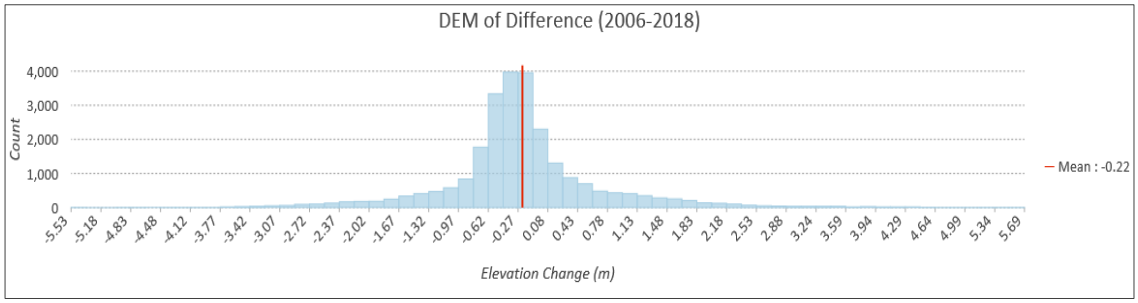

Fig. 13 Chart showing distribution of 2006-2018 DoD and average elevation change.

Elevation change was not apparent for area B based on the DoD results. However, this area was classified as an active gully in the 2001 image segmentation results. Although this was the case, it is likely a misclassification. This may be a limitation in that not all areas of barren earth indicate active gullying. Based on comparative analysis between the 2018 manually digitized gully perimeter and 2001 image classification, gully widths were larger in 2018 (Fig. 14). This lateral gully expansion over seventeen years indicates bank erosion.

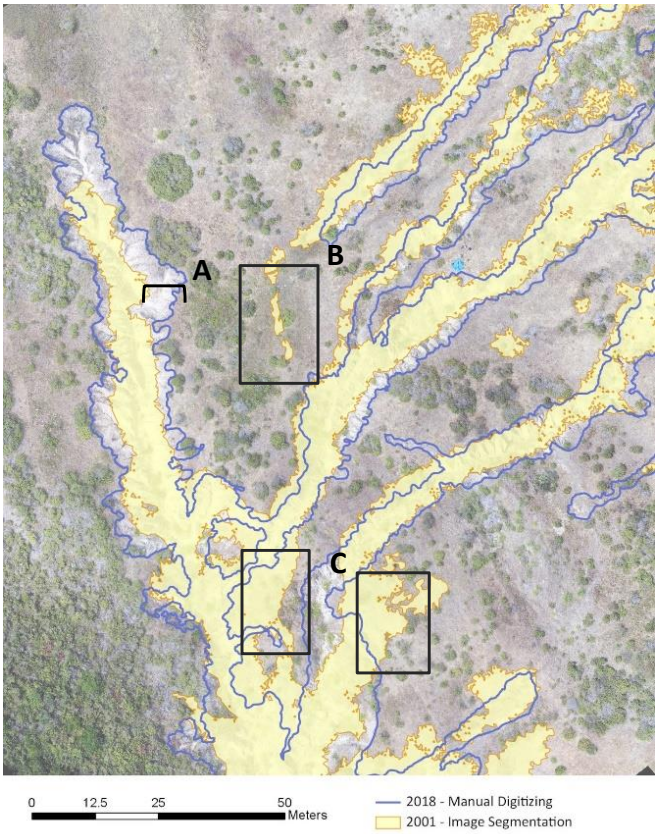

Fig. 14 Comparison of manually digitized gully edges from 2018 and image segmentation output based on 2001 imagery. Results indicate (A) lateral gully expansion, (B) gully misclassification, and (C) areas of barren soil or active erosion in 2001 that have since vegetated.

4 Discussion

The research has shown that SfM methods provided the most accurate approach for observing geomorphic gully change. These methods also proved to be the most fitting since active gully conditions were almost entirely barren soil, with minimal surrounding vegetation. The group of methods employed here can also be applied to other areas of the western Pescadero Watershed. Though not the main objective of this research, results were consistent with Swanson et al. (1989) and Spreiter (1979) who investigated reasons for gully development in the Pescadero Watersehd. This was based on aerial imagery interpretation, slope, and geology. Factors influencing gully initiation in the Pescadero Watershed include agricultural land use, Quaternary rock types, moderate slopes, and coastal scrub and grassland vegetation cover.

However, SfM methods may not be suitable for gully systems described here if they exhibit more vegetation and tree canopy cover.

DEM differencing was successfully applied for adequately monitoring the status of the gully network. The DoD approach assumed that the RMSE values followed a normal spatial distribution similar to those found by Brasington et al. (2003) and Lane et al. (2003). As discussed by Taylor (2018) in his work quantifying sediment connectivity in an actively eroding gully complex, fusing two DEM errors also assumed that both RMSE values are treated as random and independent. Experimental adjustments were applied to the DoDs using different LoD_{min} values. In some cases, as the LoD_{min} increased, 70% of the information on elevation change was excluded from the results.

Large scale geomorphic changes in erosion and deposition patterns were observed between DEM datasets, such as gully headcuts, mass movement and deep channel scour or fill. The DoDs could not capture subtle erosion changes that had elevation changes similar to the degree of DoD error. For example, the 2006-2017 DoD indicated sediment deposition at higher elevations of the gully system but did not show associated erosion (Fig. 11). These sediment deposition areas could perhaps be attributed to finer-scale bank erosion which contributes to the watershed's overall sediment budget.

5 Conclusion

Methods for accurate, effective and efficient analysis of gullies is paramount to decision making. This paper presented a combined methodology of SfM, DoD and two-dimensional analysis for sufficiently demonstrating gully erosion processes. In addition to apparent erosional patterns within the gully channels, mass-movement processes were highlighted. Historical imagery suggests that intensive land use activities in combination with moderate to steep hillslopes are principle factors influencing gully expansion.

This is the first study to apply three-dimensional analysis to illustrate gully geomorphic changes in the Pescadero Watershed. A LoD_{min} must be integrated into DoDs to consider DEM uncertainties. Additionally, two-dimensional analysis provided information where three-dimensional analysis was not feasible because too high of an error in the DEM. This research could be extended by combining a subsequent DEM from SfM and the 2018 DEM to produce a LoD_{min} that exists significantly below the

level required to capture smaller erosion processes. As DEM data sources become more accurate, uncertainties can be minimized to facilitate a higher confidence in DoD results.

The measures necessary for large gully repair and control are complex. Mitigation can be very expensive and time consuming for landowners in treatment, design and permitting. The group of methods reviewed in this study can be applied to other gullies with similar characteristics in the Pescadero Watershed. With increasing availability in accurate DEM datasets and the ability to acquire low-cost, high-resolution elevation datasets from SfM, this combined group of methods will be useful and cost-effective for analyzing multi-temporal change in gully systems. This will aid land managers in determining appropriate erosion control as well as future monitoring on the effectiveness of such efforts.

References

Bransington, J. Langham, L. Rumsby, B., 2003. Methodological sensitivity of morphometric estimates of coarse fluvial sediment transport. Geomorphology 52, 299-316.

Brown, W.M., 1973. Erosion Processes, Fluvial Sediment Transport, and Reservoir Sedimentation in a Part of the Newell and Zayante Creek Basins, Santa Cruz County, California. USGS Open File Report 73-0035.

Christian, P. and Davis, J., 2016. Hillslope gully photogeomorphology using structure-from-motion. Zeitschrift für Geomorphologie 60, Suppl. 3, 59-78.

Coe, J.A., Glancy, P.A., Whitney, J.W., 1997. Volumetric analysis and hydrologic characterization of a modern debris flow near Yucca Mountain, Nevada. Geomorphology 20, 11-28.

Conforti, M., Aucelli, P., Robustelli, G., Scarciglia, F., 2011. Geomorphology and GIS analysis for mapping gully erosion susceptibility in the Turbolo stream catchment (Northern Calabria, Italy). Natural Hazards 56, 881-898.

Environmental Science Associates, Pacific Watershed Associates, O'Connor Environmental, Inc., Albion Environmental, Inc., Dennis Jackson, 2004. Pescadero-Butano Watershed Assessment, Final Report. Prepared for Monterey Bay National Marine Sanctuary Foundation.

ESRI 2018. ArcGIS Pro. Redlands, CA: Environmental Systems Research Institute.

Frucht, S.B., 2013. Pescadero-Butano Watershed Sediment TMDL. San Francisco Bay Regional Water Quality Control Board. Project Definition and Project Plan.

Kelley, D., Loecherback, T., 2006. Challenges and Successes in Photogrammetric Approaches to LiDAR-Derived Products. MAPPS/ASPRS 2006 Fall Conference, San Antonio, Texas.

Lal, R. Mokma, D. Lowery, B., 1999. Relation between Soil Quality and Soil Erosion. Soil Quality and Soil Erosion, CRC Press, 237–58.

Lane, S.N., Westaway, R.M., Hicks, D.M., 2003. Estimation of erosion and deposition volumes in a large, gravel-bed, braided river using synoptic remote sensing. Earth Surface Process and Landforms 28, 249-271.

Marden, M., Arnold, G., Seymore, A., Hambling, R., 2012. History and distribution of steepland gullies in response to land use change, East Coast Region, North Island, New Zealand. Geomorphology 153-154, 81–90.

Ni, K., Sun, Z., Bliss, N., Snavely, N., 2010. Construction and exploitation of a 3D model from 2D image features. IS&T/SPIE Electronic Imaging, International Society for Optics and Photonics, 75330 J–75330 J.

Owens, J., Chartrand, S., Hecht, B., 2003. Geomorphic and Sediment Assessment of the Gazos Creek Watershed, San Mateo and Santa Cruz Counties, CA. Prepared by Balance Hydrologics, Inc. for the Coastal watershed Council, Santa Cruz, CA. 24p. 2003.

Pix4D, 2018. Pix4D User Manual: Professional Edition. https://support.pix4d.com/hc/en-us/sections/200591059-Manual.

Redwood City Times and Gazette, July 8, 1876. Redwood City, San Mateo County, CA.

Resource Conservation District, San Mateo County, 2017. Coastal San Mateo County Gully Erosion Report, 2017. Resource Conservation District, San Mateo County.

Shruthi, R., Kerle, N., Jetten, V., 2011. Object-based gully feature extraction using high spatial resolution imagery. Geomorphology 134, 260-268.

Snavely, N., Seitz, S., Szeliski, R., 2008. Modeling the world from internet photo collections. International Journal of Computer Vision 802, 189–210.

Spreiter, T., 1979. Factors affecting gully formation and distribution in coastal San Mateo County, California. M.S. Thesis, Stanford University, Dept. of Applied Earth Sciences.

Swanson, M.L., Kondolf, G.M., Boison, P.J. 1989. An example of rapid gully initiation and extension by subsurface erosion: Coastal San Mateo County, California. Geomorphology 2: 393-403.

Taylor, R., Massey, C., Fuller, I., Marden, M., Archidald, G., Ries, W., 2018. Quantifying sediment connectivity in an actively eroding gully complex, Waipaoa catchment, New Zealand. Geomorphology 307, 24-37.

United States Department of Agriculture (USDA), Natural Resources Conservation Service, 2017. Web Soil Survey. https://websoilsurvey.sc.egov.usda.gov/App/WebSoilSurvey.aspx

Digital Collections (1943-2001). University of Santa Cruz, University of California. McHenry Library Archives. Santa Cruz, Ca.

Vendrusculo, L., 2014. Classical gully spatial identification and slope stability modeling using high-resolution elevation and data mining technique. Graduate Theses and Dissertations, 14082. Iowa State University.

Weaver, W.E. and D.K. Hagans, 1994. Handbook for Forest and Ranch Roads. Resource Conservation District, Mendocino County.

Wheaton, J.M., Brasington, J., Darby, S.E., Sear, D.A., 2010. Accounting for uncertainty in DEMs from repeat topographic surveys: improved sediment budgets. Earth Surface Processes and Landforms 35, 136-156.

Westoby, M., Brasington, J., Glasser, N., Hambrey, M., Reynolds, J., 2012. 'Structure-from-motion' photogrammetry: A low-cost, effective tool for geoscience applications. Geomorphology 179, 300–314.

Williams, R.C., 2012. DEMs of Difference. Institute of Geography and Earth Science, Aberystwyth University. Geomorphological Techniques, Chap. 2, Sec 3.2.

Zucca, C., Canu, A., Della Peruta, R., 2006. Effects of land use and landscape on spatial distribution and morphological features of gullies in an agropastoral area in Sardinia (Italy). Catena 68, 87–95.